Pergamon

NanoStructured Materials, Vol. 10, No. 6, pp. 983-1000, 1998
Elsevier Science Ltd

0965-9773/98 $19.00 + .00

PII S0965-9773(98)00135-4

CHARACTERIZATION OF Al_2O_3 COMPOSITES WITH Mo PARTICULATES, II. DENSIFICATION AND MECHANICAL PROPERTIES

Sheng-Chang Wang and **Wen-Cheng J. Wei**

Institute of Materials Science and Engineering,
National Taiwan University, Taipei, Taiwan 106, ROC

(Accepted August 4, 1998)

Abstract—*Three processes were employed to mix MoO_3 or Mo powder with submicrometric Al_2O_3 powder in the preparation of the Mo/Al_2O_3 precursors. The first two processes employed a dissolution route which dissolved MoO_3 powder in ammonia solution, followed by spray-drying or hot-plate-drying to obtain ammonium molybdate/Al_2O_3 granules. Then, the granulated powders were reduced in H_2 atmosphere and hot-pressed to obtain Mo/Al_2O_3 composites. The third process involved mechanically mixing metallic Mo particles with Al_2O_3. The composites normally can achieve 99% relative density after hot-pressing. Microstructural results of hot-pressed composites reveal that intergranular Mo grains of micrometer size dispersed at the grain boundaries of dense Al_2O_3 matrix, and some fine grain Mo grains of nanometric size were entrapped within the Al_2O_3 grains in the composite. The four-point bending strength and the toughness of the dense composites increases 26% and 32% respectively, with the addition of Mo content, but are controlled by the uniformity of the microstructure of the composites. The hardness of the composites basically obeys the prediction of the rule of mixture. The strengthening and toughening mechanisms of the composites with respect to the microstructure are analyzed. ©1998 Acta Metallurgica Inc.*

1. INTRODUCTION

The strengthening of ceramic materials has been an important issue to the engineering applications. The methods frequently reported in literature to strengthen ceramics can be classified as either grain size reductions (1) or residual stress introduction by the addition of second phase (2).

According to the Petch relation (3), the finer the grain sizes, the better the strength of materials can be increased. The relation can be expressed:

$$\sigma_f = \sigma_0 + k_1 d^{-1/2} \qquad [1]$$

where σ_f is the yielding strength, σ_0 is a constant representing the stress for dislocations glide on

the slip system, d is the grain size and k is a material parameter which is formulated as $\left(\frac{3\pi\gamma E}{1-\nu^2}\right)$. The parameter k is in fact a function of the surface energy γ, elastic modulus E, and Poisson's ratio ν. But for brittle materials, such as ceramics, it is difficult to observe the dislocation glide at room temperature. However, equation [1] reveals that the fracture strength of materials may increase with the decrease of the grain size if the dimension of intrinsic defects is in the same range as that of the grain size (4). The Griffith equation states that the fracture strength is inversely proportional to the square root of the flaw size (or grain size). Consequently, the reduction of the grain size by processing efforts may lessen the crack size and improve the strength of ceramic materials.

In addition to the reduction of grain size, the inclusions (either in fibrous or particulate form) of composite materials can strengthen the materials by inducing residual stresses acting near the interfaces between inclusion and matrix. Compressive stress may compensate tensile forces or deflect a crack propagated through the stress zone, and finally improve the strength of the composites. The increase in toughness is also beneficial for the increase of fracture strength (σ_f).

TABLE 1
Literature Reported Mechanical Properties of Al_2O_3/Mo Composites.
The shape, fabrication method, and volume content of Mo inclusions, the values of maximum strength, and maximum toughness (fracture energy) ratio are included.

Mo Shape	Fabrication Method	Maximum Strength Ratio	Maximum toughness (fracture energy) ratio	References
Particulate	ball milled, reduction 5/6 vol.% sintering	1.2	5 vol.%	McHugh et al., 1966 (6)
Fiber	hot pressing	—	(250) 12 vol.%	Simpson et al., 1971 (7)
Particulate	hot pressing	1.2 3 vol.%	1.3 5 vol.%	Rankin et al., 1971 (5)
Elongated and particulate	ball milled hot presing	1.5 5 vol.%	1.8 20 vol.%	Nawa et al., 1994 (8)
Flake	ball milled, hot pressing	2.5 20 vol.%	1.3 20 vol.%	Waku et al., 1995 (9)

The Mo/Al_2O_3 composites have been investigated for two decades (5). The summary of these research efforts including the fabrication method, Mo shape, maximum strength and toughness improvements are shown in Table I. Most of the work reported in the literature started from metallic Mo fibers or particulate. The strengthening effects due to the presence of the Mo phase result in an improvement of from 20 to 150%. This study selected a chemical route for the preparation of Mo-species, and finally, to produced two series of dense Al_2O_3 composites with the Mo additive of sizes ranging from nanometer to submicrometer. The microstructure and mechanical properties of three Mo/Al_2O_3 composites were examined, revealing the strengthening mechanism and the rules of the Mo phase.

2. EXPERIMENTAL PROCEDURE

2.1 Sample Preparation

The Mo was prepared from two different sources, either MoO_3 powder (99.95% pure, Climax Molybdenum Co. USA), or metallic Mo powder (Climax Specialty Metals, USA). Submicron Al_2O_3 powder (99.7% pure, A-16SG, Alcoa Industrial Chemical, USA) was used as the matrix material in this study.

A dissolution, then spray-drying process was used in our previous report (10) for the preparation of molybdate/Al_2O_3 granules. The spray dried granules were then subjected to H_2 reduction to form a molybdenum phase at 600°C ~ 900°C.

There are two different ways to produce the Mo/Al_2O_3 composites for comparison. One is to mechanically mix Mo and Al_2O_3 powder. Instead of using spray drying, the alternative process is to dissolve MoO_3 powder in the ammonia solution and then dry on a hot plate. The dried molybdate/Al_2O_3 can be granulated and reduced in H_2 atmosphere as seen in the sample.

The reduced or mixed Mo/Al_2O_3 powders were hot pressed (High-multi 5000, Fujipempa Kogyo Co., Japan) in a graphite die of 50 mm diameter. The hot pressing conditions were 1400°C with an applied uniaxial pressure of 30 MPa for 1 hr in a vacuum atmosphere.

2.2 Characterization

The densities of hot-pressed composites were measured by Archimedes' method. The microstructure of the sintered composites was analyzed by SEM (Philips 515, Philips Co., Netherlands), TEM (JEOL 100CXII, Japan), and HRTEM (JEOL FX-4000E, Japan). The fracture strength was measured by a four-point bending method conforming to ASTM C1161. Rectangular test bars with dimensions 3 x 4 x 35 mm were cut from the hot-pressed cylindrical specimens using a diamond blade saw, and finally surface ground with a 325 grit diamond wheel. The specimens for fracture toughness and Vicker's hardness were carefully polished. The fracture toughness was estimated by the micro-indentation method with the equation given by Marshall and Evans (11), Vicker's indentation with a load of 196 N and 9.8 N was used for the measurements of toughness and hardness, respectively.

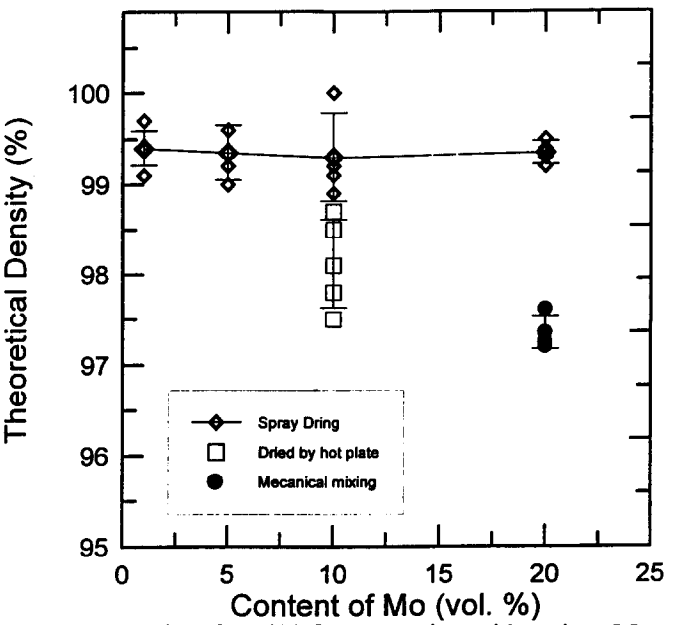

Figure 1. Relative density of Mo/Al_2O_3 composites with various Mo contents and prepared by three processes. The composites were reduced at 900°C in H_2 and hot pressed at 1400°C for 1 hr in vacuum.

Figure 2.TEM micrographs of Mo/Al_2O_3 composites. The samples were reduced at 900°C in H_2 and then hot pressed at 1400°C for 1 hr in vacuum (a) 1 vol.%, (b) 5 vol.%, (c) 10 vol.%, and (d) 20 vol.%.

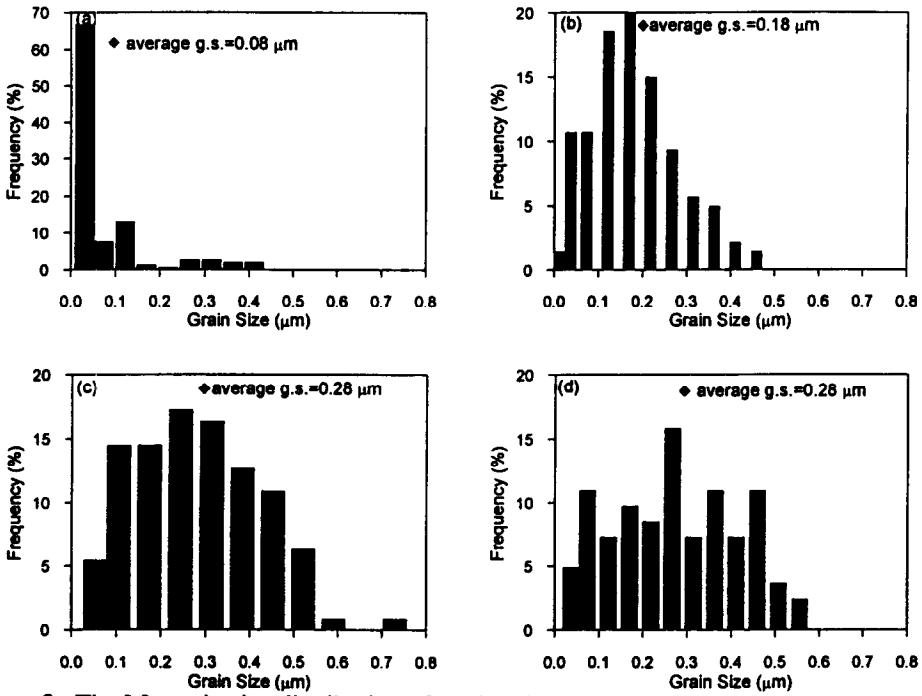

Figure 3. The Mo grain size distribution of Mo/Al_2O_3 compsoites prepared from 900°C reduced powder. The samples were hot pressed at 1400°C (a) 1 vol.%, (b) 5 vol.%, (c) 10 vol.%, and (d) 20 vol.%.

3. RESULTS

3.1 Densification and Microstructure

The hot-pressed density of the Mo/Al_2O_3 composites with various Mo contents is shown in Figure 1. All the composites were hot-pressed at 1400°C in a vacuum for 1 hr. Only the density of the composites made by spray drying can achieve ≥99.0% theoretical density. The relative density of the other samples by hot plate drying and directed mixing powders achieve 98±0.6% and 97.2±0.2% T.D., respectively.

The TEM micrographs of Mo/Al_2O_3 composites are shown in Figure 2. In addition to some dispersed porosity, the grain structure of the matrix phase and inclusion are noted. Due to the atomic number of Mo being far higher than Al_2O_3, the scattering contrast results in a black feature for Mo grains and gray for Al_2O_3 grains.

Either intergranular and intragranular Mo grains were found in the micrographs of these composites. The statistical result of the Mo grain size are shown in Figure 3. About 80% Mo grains were found entrapped in the Al_2O_3 grains of the 1 vol% Mo composite (Figure 2(a)). Most of the intragranular Mo grains are less than 0.1 μm and in an average grain size of 80 nm. But the Mo grains become 0.28 μm in 20 vol% Mo composite, and mostly located at grain boundaries, as shown in Figure 2(d).

Figure 4 shows several marked intragranular Mo grains which were trapped in an Al_2O_3 grain. The TEM micrograph reveals that the average Al_2O_3 grain size containing these ultrafine

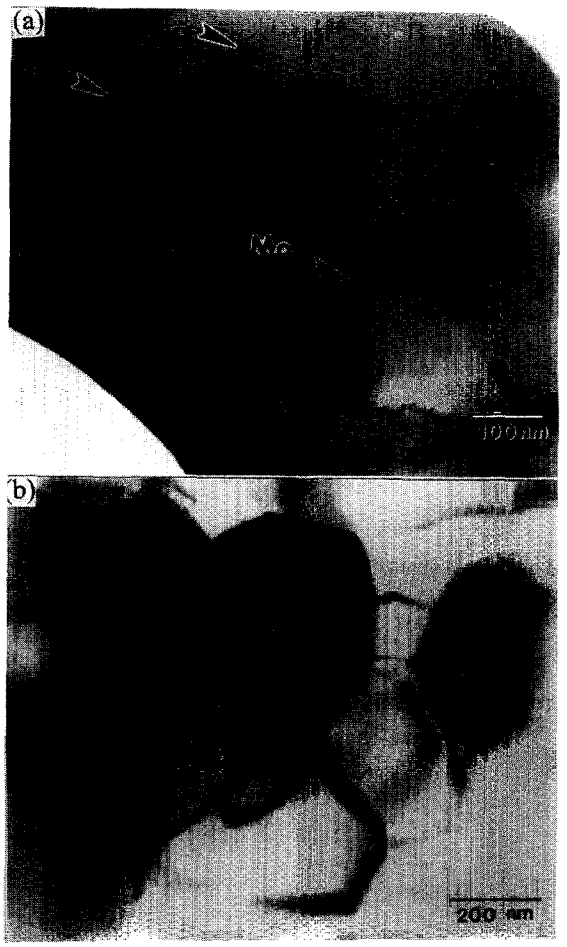

Figure 4. TEM micrographs of (a) intragranular Mo inclusions in Al_2O_3 of 1 vol.% Mo/Al_2O_3 composite, and (b) the dislocations within intergranular Mo grain in 20 vol% Mo/Al_2O_3 sample.

(<100 nm) Mo inclusions is larger than those Al_2O_3 grains without any intragranular Mo inclusions. The average grain size of the intragranular Mo phase is 30 nm, which approximately equals the original size after a 900°C reduction (10). This implies that Mo particles stop coarsening when they are entrapped in the Al_2O_3 grain during sintering.

A great difference is noted for the intergranular Mo phase which is normally in the sizes 0.2 to 0.6 μm. The interior of these Mo grains, as shown from the TEM micrograph in Figure 4(b), is full of dislocations which may have been induced by thermal stress during cooling from the sintering temperature. The possible cause for the formation of the dislocations will be discussed in the section 4.

The microstructures of Mo/Al_2O_3 composites prepared by hot plate drying and mechanical mixing are shown in Figure 5. Many plate-like Mo agglomerates are dispersed in the composite

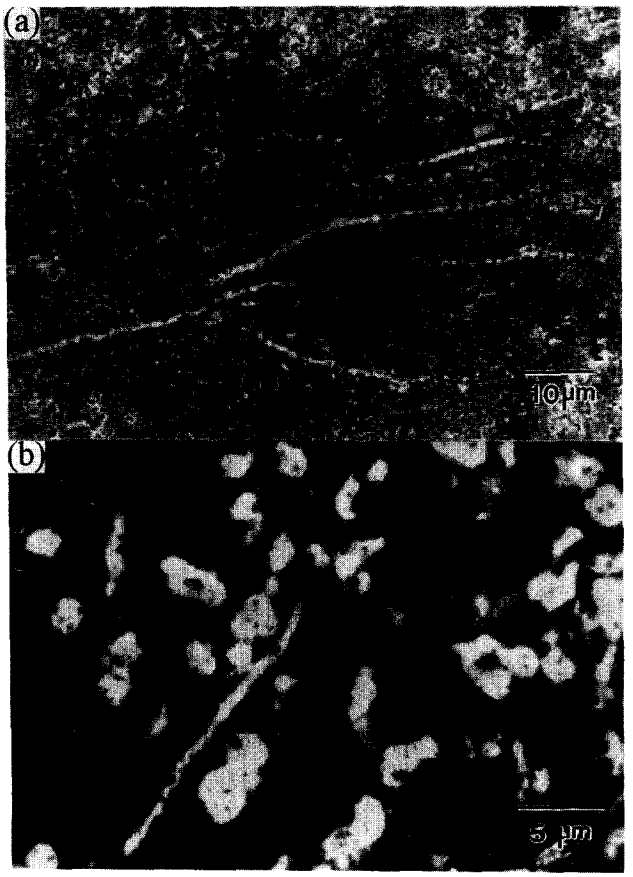

Figure 5. SEM micrographs of unetched polished surfaces of (a) 10 vol.% Mo/Al_2O_3 composites prepared by hot plate drying, and (b) 20 vol.% Mo/Al_2O_3 composites prepared by mechanical milling.

(Figure 5(a)) prepared by hot plate drying. The cluster of the agglomerates is about 20~30 μm long, 1 μm thick. The drying procedure of the processing method cannot make the molybdate solution homogeneously be precipitated. Instead, some flaky features of Mo phase are formed during drying and preserved after hot-pressing. Similarly, there are also flaky and coarser Mo grains in composites prepared by the mechanical mixing of Mo and Al_2O_3 powder, as shown in Figure 5(b). The flaky Mo particles were deformed during the ball milling by hard TZP media. Because the coarse Mo phase disperses in the matrix, the sintering density of the composites is suppressed.

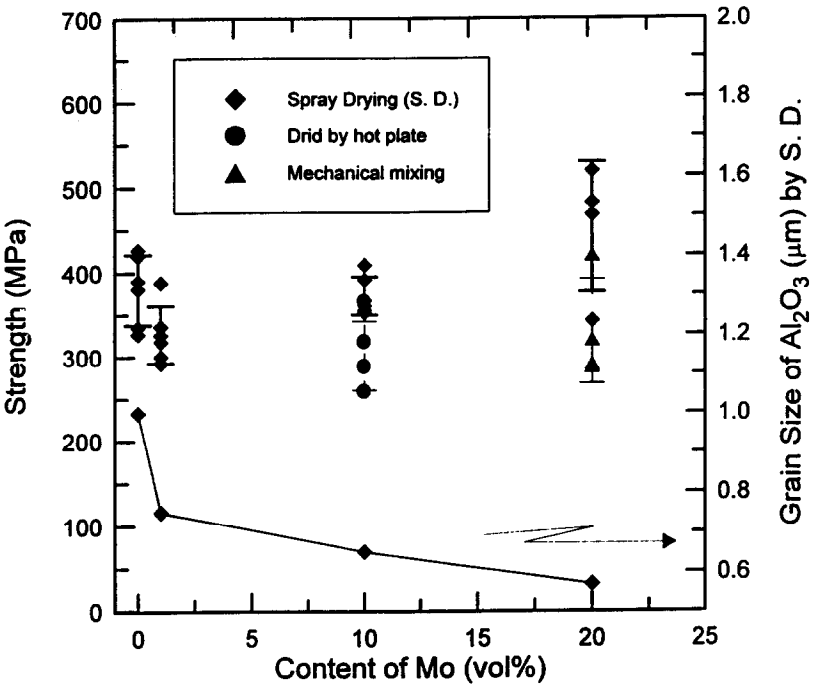

Figure 6. Four-point bending strength and Al_2O_3 grain size versus the vol.% of Mo. The compoite prepared from 900°C reduced powder, and hot pressed at 1400°C for 1 hr in vacuum.

3.2 Mechanical Properties of Various Mo/Al_2O_3 Composites

The four-point bending strength of the Mo/Al_2O_3 composites and the grain size of Al_2O_3 matrix varied with the volume content of Mo up to 20 vol% are shown in Figure 6. The fracture strength increases with the addition of Mo phase. Among these, the 10 vol.% Mo/Al_2O_3 composite has a maximum strength of 530 MPa. The strength is 40% greater than a monolithic Al_2O_3 prepared under the same condition. The other series of the composites have a lower strength, either 346 MPa or 300 MPa, respectively. The cause of a strength lower than the samples prepared by dissolving-precipitation/spray-drying may be due to the lower sintering density of the two composites.

The fracture toughness of the composites is shown in Figure 7. The average fracture toughness of a monolithic Al_2O_3 by hot pressing is 3.4 MPa.$m^{1/2}$ which is 32% lower than the best Mo/Al_2O_3 composites (4.5 MPam$^{1/2}$) made by the dissolving-precipitation/spray-drying process, which increases slightly with the addition of Mo phase. The more the added Mo, the better the toughness. However, the fracture toughness of the composites prepared by either mechanical mixing or dried by hot plate (6.0 or 4.7 MPa.$m^{1/2}$) is higher than that prepared by the spray drying method. This is because that the coarse Mo grains and flaky Mo agglomerates cause crack deflection and bridging effects, as shown in Figure 8(c) and (d), which are more apparent than in the spray-dried/hot-pressed composite (Figure 8(b)).

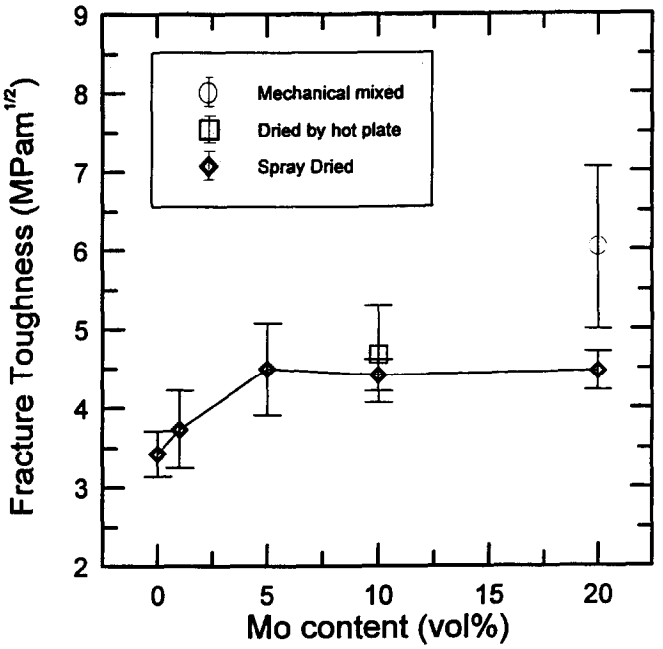

Figure 7. Variation of toughness with Mo contents for Mo/Al_2O_3 composites prepared from three methods and hot pressed at 1400°C for 1 hr in vacuum.

SEM pictures of fracture surface for monolithic Al_2O_3 and Mo/Al_2O_3 composites with Mo from 1 to 20 vol.% are shown in Figure 9. Shell cleavage often occurred on the surface of micron-sized Al_2O_3 grains. This is an evidence of a transgranular fracture mode. But the mode is likely of an intergranular type in the finer Al_2O_3 grains. The fracture type of the composites should be a mixed mode of intergranular and transgranular, depending upon the matrix grain size and the volume content of Mo inclusion.

The variation of Vicker's hardness of the composites with Mo content is shown in Figure 10. The line presents the hardness calculated by the rule of mixture, also shown in the figure. The hardness of monolithic Al_2O_3 and Mo is 18.6 GPa (12) and 2.1 GPa (13), respectively. Because the hardness of Mo phase is lower than that of Al_2O_3, the hardness of the composites shall decrease with increases of Mo content. In this study, the hardness approximately obeys the rule of mixture.

4. DISCUSSION

4.1 Evolution of Mo and Al_2O_3 Phases in Dense Composites

The size distribution of Mo grain with different Mo contents is shown in Figure 3. The average grain size of Mo phases in the 5 vol% Mo composites is larger (0.2 μm) than that (80 nm) in 1 vol% Mo composite. The fraction of the intragranular Mo grains is also reduced from 80% (of 1 vol% Mo composite) to 35% (of 5 vol% Mo composite). The fraction of intragranular Mo in

Figure 8. SEM micrographs of crack morphology around the Vicker's indentation for 20 vol.% Mo/Al_2O_3 composites fabricated by spray-drying: (a) entire indentation, (b) propagation of crack, (c) 10 vol.% Mo/Al_2O_3 composite prepared by hot-plate drying, and (d) 20 vol.% Mo/Al_2O_3 composite prepared by mechanical mixing.

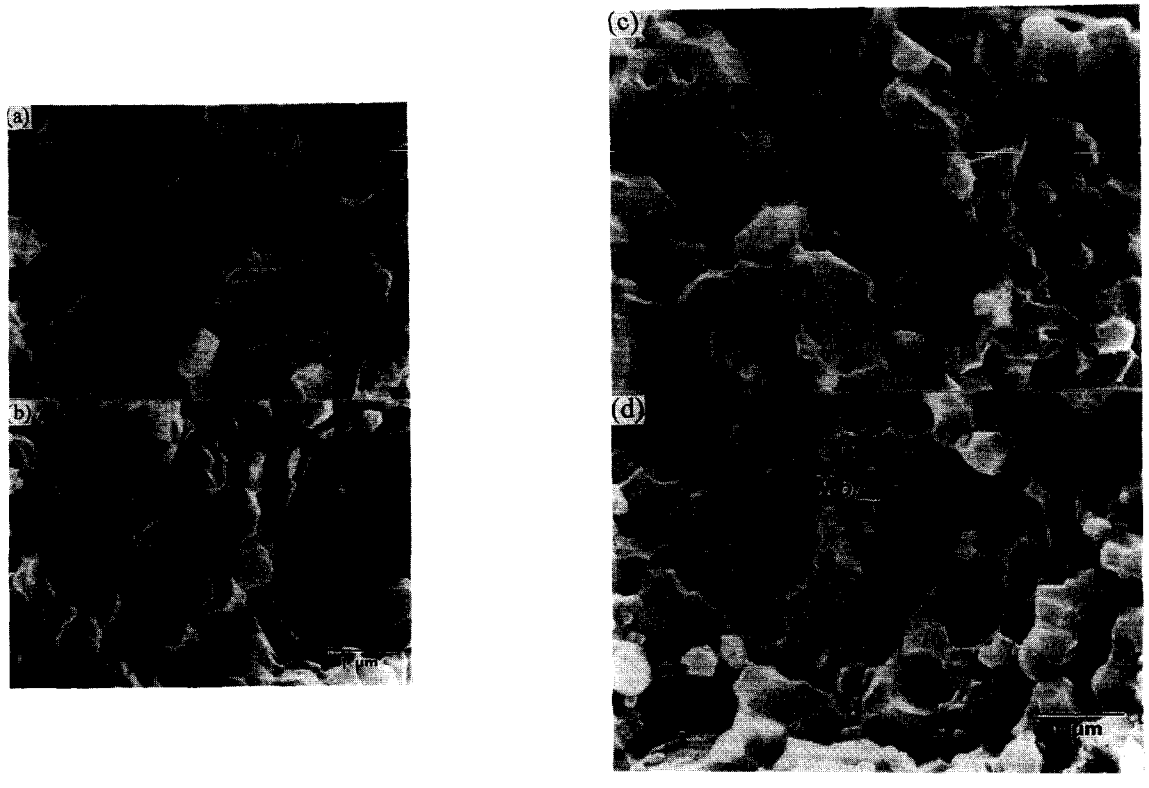

Figure 9. SEM micrographs of the fracture surfaces of Mo/Al_2O_3 composites hot pressed at 1400°C for 1 hr in vacuum: (a) 0 vol.%, (b) 5 vol.%, (c) 10 vol.%, and (d) 20 vol.% Mo content.

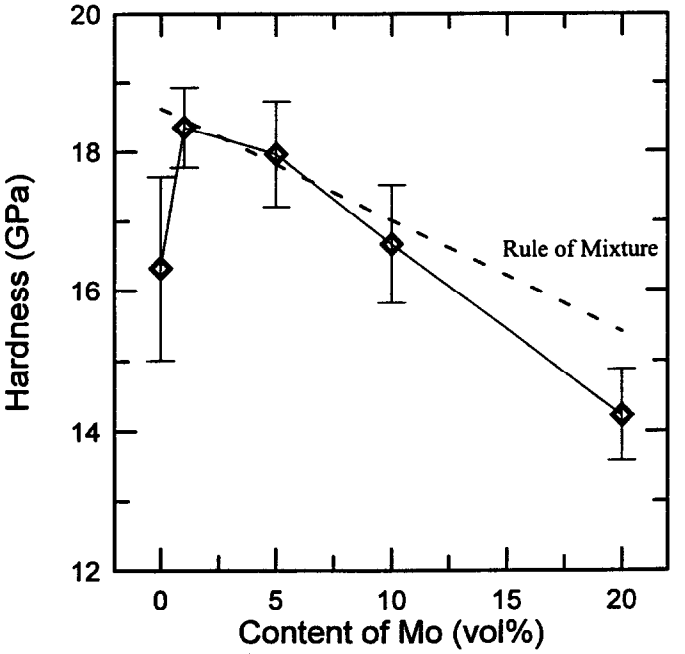

Figure 10. Vicker's hardness plotted as a function of Mo content in Mo/Al_2O_3 composites hot pressed at 1400°C for 1 hr in vacuum.

composites reduced further to 30% and the average grain size became 0.29 μm in the 10 vol% Mo composite. The percolation theory (14) depicts that if the fraction of the second phase is larger than 16 volume percent, then the second phase could interconnect and become a three-dimensional network structure. In other words, some of the Mo grains would interconnect. Due to the Mo grains in the 20 vol.% Mo/Al2O3 composite being greater than the threshold volume (16%), the fraction of the intergranular Mo phases increases to 84% and the average grain size grows to 0.29 μm.

The grain size of the Al_2O_3 in Mo/Al_2O_3 composites varied with the volume fraction of Mo phases is plotted in Figure 11. The data fitted with lines calculated with the Zener (15) and topological models (14) are also shown in the figure. In fact, the slope of two lines (Figure 11) represents the relation of the matrix grain size (G) to the volume fraction (f) of the second phases. Zener (15) proposed a model which also considered the grain size (r) effect of non-reactive, spherical inclusions on the ultimate grain size (G_L) of a matrix. This shows that:

$$G_L = K\frac{r}{f} \qquad [2]$$

where K is a constant of about 4/3 (16). Zener's model expresses that the grain size of a matrix is limited inversely proportional to the amount of inclusion, in other words $G \propto f^{1}$. The solid line in Figure 11 appropriately represents four data points. However, the topological model describing the powder index is -1/3, which means $G \propto f^{-1/3}$. This value is four times greater than the slope

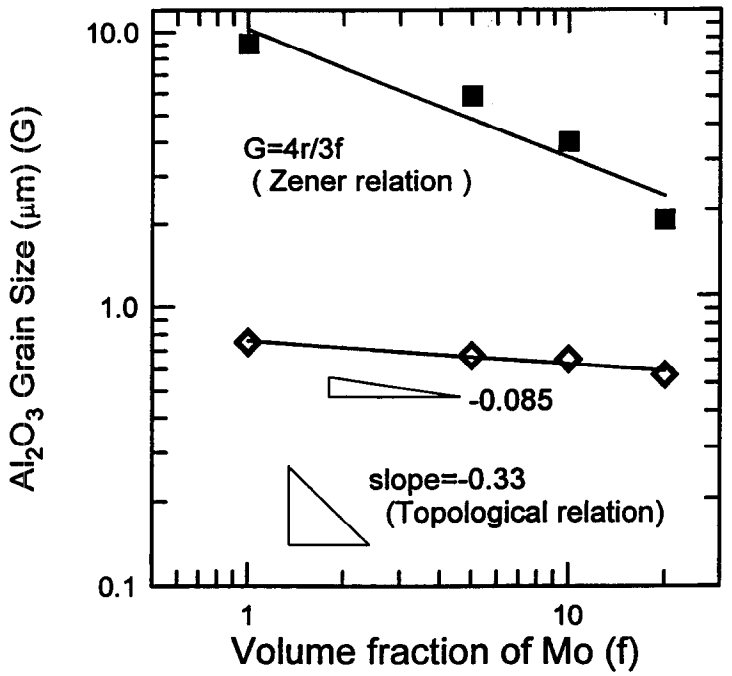

Figure 11. Grain size of Al_2O_3 as a function of the volume percent of Mo. The lines show the predictions by the Zener and topological equilibrium models. The experimental data are plotted as squares.

(-0.085) of the line in Figure 11. From the above discussion, the limiting grain size of the Al_2O_3 is beyond the prediction of the topological model. The Mo phase may change its grain size by coarsening during hot-pressing. Additionally, the spatial distribution of Mo phases is not random enough to allow the intergranular and intragranular Mo phases to exist simultaneously in the matrix.

Additional discussion for the differentiation of the rules of various inclusions was given by Harmer *et al.* (17,18). It concerned the fraction (ϕ) of the second phases at the grain boundary of the matrix phase for the retardation of the grain boundary movement. The previous result in Figure 11 is re-plotted by using the volume fraction of Mo phase at grain boundaries as the abscissa, shown in Figure 12. The data in the figure can be fitted by a line which holds the relationship as:

$$G = 2.24\ \phi^{-0.17} \qquad [3]$$

where G is the grain size of matrix Al_2O_3 in a unit of μm. The volume fraction (ϕ) of the Mo phase appearing at the grain boundaries is between 25% to 90%. The grain size of all four samples in Figure 12 is less than 1.0 μm. The retardation of the grain growth of the Al_2O_3 matrix is evident within the experimental range of ϕ. It is worthwhile testing the grain growth at higher temperatures (>1400°C) or to prepare the composite with less Mo at grain boundaries.

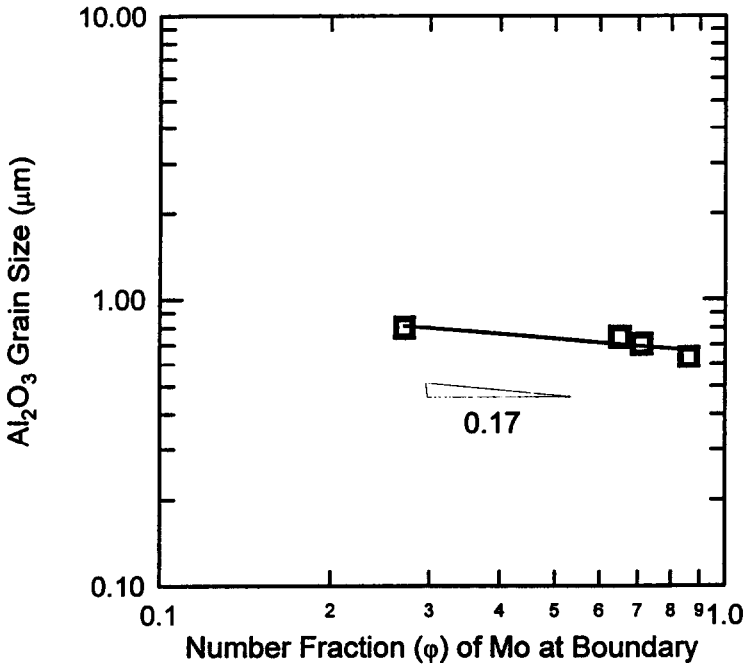

Figure 12. Al_2O_3 matrix grain size as a function of the fraction of Mo at grain boundary.

In the early stage of the sintering, all the Mo grains are at the grain boundary of Al_2O_3 grains. If the amount of added Mo is lower, the dragging force exerted by the Mo particles to the Al_2O_3 grain boundary is relatively small. As a consequence, the grain boundary moves rapidly because of the driving of the specific surface energy. Once the Mo grains are enclosed by Al_2O_3 grains, and the grain size of the Mo inclusions stop growing. The evidence is clearly observed from that the size of the intragranular Mo is not growing after H_2 reduction and through sintering steps.

4.2 Thermal Stress and Strengthening Mechanism

Stresses of composites can be normally generated from a thermal process. The scale of the thermal stresses depends on the inclusion volume fraction, inclusion geometry and size, thermal mismatch ($\Delta\alpha$), the temperature interval (ΔT), and modulus ratio. According to the theory proposed by Seleing (19), a composite consisting of elastic spheres with a uniform size embedded in an infinite elastic continuum and cooled down from a high temperature may exert a radial stress (σ_{rp}) and tangential stress ($\sigma_{\theta p}$) which will produce in the spherical inclusion:

$$\sigma_{rp} = \sigma_{\theta p} = -P = \text{Constant, where } P = \frac{\Delta\alpha \cdot \Delta T}{\frac{(1+\nu_m)}{2 \cdot E_m} + \frac{(1-2\nu_p)}{E_p}} \quad [4]$$

While the stresses in the matrix are a function of distance (r) away from the center of the spherical inclusion.

$$\sigma_{rm} = -P\left(\frac{R}{r}\right)^3 \quad [5]$$

and

$$\sigma_{\theta m} = \frac{P}{2}\left(\frac{R}{r}\right)^3 \quad [6]$$

where the subscripts p and m represent particle and matrix, respectively, and R is the radius of inclusion.

The formation of cracks at the interface is critical, and can be judged by the bonding strength and maximum tensile stresses at the interface. If the inclusion size is larger than a critical size d_c, the thermal stress can produce microcracks. The types of the microcracks can be categorized as two types. In general, an inclusion in a smaller thermal expansion coefficient (CTE) than the matrix, $\alpha_p < \alpha_m$, would produce a compressive stress inside the inclusion, a radial compressive stress and tangential tensile stress in the matrix. If the $\sigma_{\theta m}$ is larger than the fracture strength σ_{fm}, a radial crack would be produced in the matrix but near the interface. When the fracture occurs, the crack will propagate along the radial direction and create a transgranular fracture mode. Conversely, if $\alpha_p > \alpha_m$, a tangential crack would be produced around the inclusion.

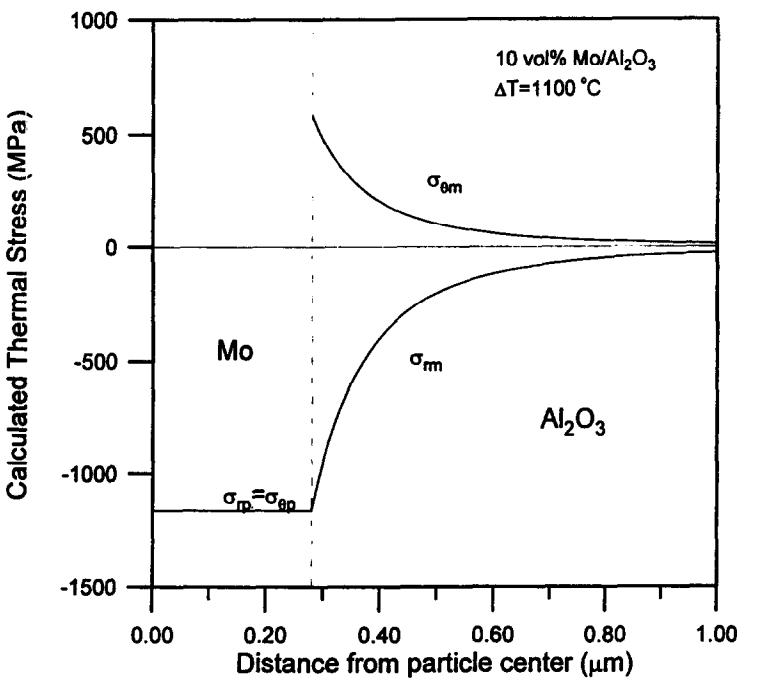

Figure 13. Schematic distribution of thermal stresses in 10 vol.% Mo/Al_2O_3 composites for a $\Delta T = 1100°C$.

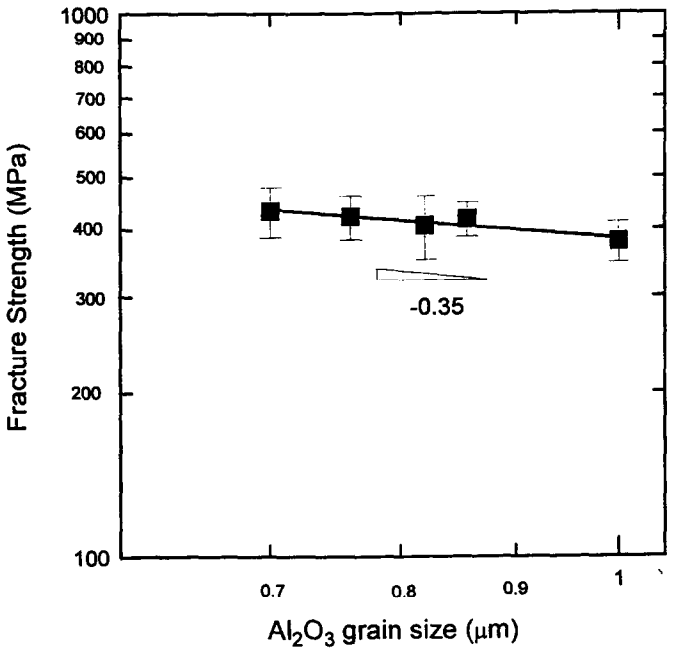

Figure 14. Orowan relation of fracture strength vs. Al_2O_3 grain size of Mo/Al_2O_3 composites.

The thermal expansion coefficient of Al_2O_3 and Mo is 8.4 x 10^{-6} and 5.4 x 10^{-6}/ K, respectively (12,13). When the composite is cooled down from a high temperature (*e.g.* 1400°C), the thermal stress would be induced at the interface of Mo and Al_2O_3. Assume the elastic modulus and Poisson's ratio of monolithic Al_2O_3 and Mo to be 400 GPa, 328 GPa, 0.25, and 0.29, (12,13), respectively. If the ΔT is equal to 1100°C, the stress distribution of a 10 vol.% Mo/Al_2O_3 composite can be calculated by equation [4] and shown in Figure 13. The thermal stresses (σ_{rp} and $\sigma_{\theta p}$) in the Mo inclusions is -1.16 GPa. Because the thermal expansion coefficient of Al_2O_3 is greater than Mo, so a uniform compressive stress is acting in the Mo particle. The matrix is under a radial compressive stress (σ_{rm}) and a tangential tensile stress ($\sigma_{\theta m}$) varying in the distance from the center of an Mo particle.

When the composites exert stresses by thermal effects, the dislocations found in Mo grains might form and glide to consume the fracture energy. In addition, the tangential tensile stress in the alumina would attract cracks propagating to the Mo phase during the extension of the crack. The reasons are that the inclusions change the fracture mode from a mixture of an inter/ transgranular mode to a pure transgranular mode while there is a tensile hoop stress around the inclusions. Both mechanisms might improve the mechanical properties of the composites.

According to Davidge's theory (20), if the side of second phase is larger than a critical size, microcracks might be produced in the composites. The critical size of an inclusion (d_c) can be estimated by the following equation:

$$d_c \geq \frac{8\gamma_s}{P^2\left[\frac{(1-\nu_m)}{E_m}+\frac{2(1-2\nu_p)}{E_p}\right]} \quad [7]$$

where γ_s is is the surface energy. Because the surface energy of normal Al_2O_3-metal is between 1.5-2.3 (J/m^2) (21), we assume the interface energy of Al_2O_3-Mo to be γ=2.0 J/m^2. Equation [7] gives $d_c \geq 2.09$ μm. Investigating our SEM results, it can be seen that all the grain size of Mo in the composites are less than 1 μm. Therefore, there will be no microcracks observed in the composites, as shown in the TEM micrographs in Figures 2 and 4.

The increase of the fracture strength is reported in Figure 6 due to the refinement of Al_2O_3 grain size, which is attributed to the inhibition of the boundary movement resulting from the presence of Mo particles. The relation of the strength and Al_2O_3 grain size can be expressed as an Orowan equation (Figure 14) as below.

$$\sigma_f = 384 \cdot d^{-0.35} \text{ (MPa)} \quad [8]$$

where d is the grain size of Al_2O_3 in an unit of μm.

It has been shown that the strengthening of the Mo/Al_2O_3 composites can be due to (i) the reduction of the grain size of matrix phase; or (ii) the increase of toughness of the composites. Both are contributed by the addition of Mo phase which may play the role of boundary inhibitor and/ or generate favorable thermal stresses for the deflection of cracks.

5. CONCLUSION

The sintered density of the composites prepared by a chemical route (dissolution and precipitation) is 99.4% theoretical density by hot-pressing sintered at 1400°C for 1 hr at 25 MPa in a vacuum. But the composites prepared by two other methods, either mechanically mixing Mo and Al_2O_3 powder directly or dissolved MoO_3 powder to the ammonia solution and dried on the hot plate, are only 97.3% and 98% T.D., respectively.

The intragranular and intergranular Mo grain are in 30 nm and a few hundred nm scales, respectively. The average grain size of Mo increases with the additional content of Mo and the Mo grain can inhibit the grain growth of the Al_2O_3 matrix. Even with 20% Mo at grain boundaries, the Al_2O_3 grain size can be controlled to less than 1.0 μm. The relationship can be expressed by the Zener's model, but not the topological model.

The maximum thermal stress in the Mo grain calculated from the theory is compressive and may be as high as 1.16 GPa. The critical Mo size that will produce microcracks is 2.9 μm. In this study, no Mo grain, neither intergranular nor intragranular is smaller than the value, and therefore no interfacial cracks are observed by SEM or TEM.

The toughness of the composites increase with the addition of Mo, and shows a 32% improvement. The toughening mechanism is the combination of cracks deflection, crack bridge, and the pull-out of metallic grains. The hardness of the composites obeys the rule of mixture.

The fracture strength of Mo/Al_2O_3 composites increases with the increase of Mo content. The maximum strength of the composites is 26% greater than a monolithic Al_2O_3. The strength-

ening mechanism is mainly the refinement of the matrix grain and the improvement of toughness due to the addition of Mo inclusions. The relationship of the fracture strength (σ_f) and grain size (d) can be expressed as: $\sigma_f = 384 \cdot d^{-0.35}$ (MPa).

The sintering density and strength of the composites made by mechanically mixing or hot-plate drying are lower than that prepared by chemical precipitation. However, the toughness of the composite made by the mechanical mixing or hot plate drying is better.

ACKNOWLEDGMENT

The authors like to thank the funding from National Science Council in Taiwan in a contract number NSC87-2216-E-002-034.

6. REFERENCES

1. Lange, F.F., *Journal of the American Ceramic Society,* 1989, 72, 3.
2. Pezzotti, G., Sergo, V., Ota, K., Sbaizero, O., Muraki, N., Nishida, T. and Sakai, M., *Journal of the Ceramic Society of Japan,* International Edition, 1996, 104, 473.
3. Petch, N.J., *Journal of Iron and Steel Institute,* 1953, 174(1), 25.
4. Carniglia, S.C., *Journal of the American Ceramic Society,* 1976, 55(7), 1167.
5. Rankin, D.T., Stiglich, J.J., Petrak, D.R. and Ruh, R., *Journal of the American Ceramic Society,* 1971, 54(6), 277.
6. McHugh, C.O., Whalen, T.J. and Humenik, M., Jr., *Journal of the American Ceramic Society,* 1966, 49(9), 486.
7. Simpson, L.A. and Wasylyshyn, A., *Journal of the American Ceramic Society,* 1971, 54(1), 56.
8. Nawa, M., Sekino, T., Niihara, K., *Journal of Materials Science,* 1994, 29, 3185.
9. Waku, Y., Suzuki, M., Oda, Y and Kohtoku, Y., *Journal of Ceramic Society of Japan,* 1995, 103, 702.
10. Wei, W.C.J., Wang, S.C., Cheng, F.H., *Nanostructured Materials,* 1998, 10(5), in press.
11. Marshall, D.B. and Evan, A.G., *Communication of the American Ceramic Society,* 1981, 11, C-182.
12. German, R.M., *Powder Metallurgy Science,* Metal Powder Industrial Federation, 2nd Ed., 1994, p. 452.
13. Lide, D.R., *CRC Handbook of Chemistry and Physics,* 72nd ed., CRC Press, Inc., 1992.
14. McLanclan, D.S., Blaszkiewicz, M. and Newnham, R.E., *Journal of the American Ceramic Society,* 1990, 73(8), 2187.
15. Zener, C., as communicated by C.S. Smith, *Transactions of the American Institute of Mining and Metallurgical Engineering,* 1948, 175, 15.
16. Chiang, Y.M., Birini, D. III, Kingery, W.D., *Physical Ceramics—Principles for Ceramic Science and Engineering,* John Wiley & Sons, 1997, p. 380.
17. Stearns, L.C. and Harmer, M.P., *Journal of the American Ceramic Society,* 1996, 79(12), 3013.
18. Stearns, L.C. and Harmer, M.P., *Journal of the American Ceramic Society,* 1996, 79(12), 3020.
19. Selsing, J., *Journal of the American Ceramic Society,* 1961, 44(8), 419.
20. Davidge, R.W. and Green, T.J., *Journal of Materials Science,* 1968, 3, 629.
21. Kingery, W.D., Bowen, H.K., Uhlmann, K.R., *Introduction to Ceramics,* John Wiley & Sons, 2nd ed., 1976.